Molecular Crystals and Liquid Crystals

ISSN: 1542-1406 (Print) 1563-5287 (Online) Journal homepage: http://www.tandfonline.com/loi/gmcl20

Induction of chiral phases in originally achiral hydrogen-bonded dimer liquid crystals

Minko Petrov, Boyko Katranchev & Peter Rafailov

To cite this article: Minko Petrov, Boyko Katranchev & Peter Rafailov (2016) Induction of chiral phases in originally achiral hydrogen-bonded dimer liquid crystals, Molecular Crystals and Liquid Crystals, 641:1, 95-105, DOI: 10.1080/15421406.2016.1185571

To link to this article: http://dx.doi.org/10.1080/15421406.2016.1185571

Published online: 15 Dec 2016.

MOLECULAR CRYSTALS AND LIQUID CRYSTALS
2016, VOL. 641, 95–105
http://dx.doi.org/10.1080/15421406.2016.1185571

Taylor & Francis
Taylor & Francis Group

Induction of chiral phases in originally achiral hydrogen-bonded dimer liquid crystals

Minko Petrov, Boyko Katranchev, and Peter Rafailov

G. Nadjakov Institute of Solid State Physics, Bulgarian Academy of Sciences, Sofia, Bulgaria

ABSTRACT

We investigated the seventh homologues of the hydrogen bonded in dimers liquid crystals p,n alkyloxybenzoic acids (7OBA), which in its pristine state displays achiral nematic (N) and smectic C (S_C) states. The mixture of this liquid crystal with nanoparticles, expressing various shapes and sizes, where the liquid crystal serves as a matrix, introduces new optical and electrooptical properties of the composite material. We concentrated on the mixture 7OBA with single wall carbon nanotubes (SWCNTs), which exposes a set of chiral and ferroelectric states, including the unique one (smectic C_G) state, which do not appear in the pristine achiral 7OBA. On the base of polarization microtextural, thermal and polarization spectroscopic (FT far infra red-FT FIR and microRaman) analyses we present a qualitative model of the smectic C_G state in low-molecular dimeric liquid crystals.

KEYWORDS

dimer liquid crystals; carbon nanotube; chirality; ferroelectricity

1. Introduction

The correlation between the liquid crystalline behaviour of p,n alkyloxybenzoic acids (nOBA's) and their physical properties has been the topic of many investigations after the first synthesis of these materials [1,2]. The first hydrogen-bonded complexes exhibiting LC behaviour resulted from the dimerization of aromatic carboxylic acids was presented in [3]. The formation of the mesogen phases in those substances depends on the capability of the nOBA's molecules to form hydrogen bonded dimers. (see [4–6]).

Following the first and well-established examples of liquid crystal formation through the dimerization of aromatic carboxylic acids, several classes of compounds have been prepared by the interaction of complementary molecules, the liquid crystal behaviour of which is crucially dependent on the structure of the resulting supramolecular system. The dimerization ability of nOBA is the most used for preparation of the supramolecular hydrogen bonded liquid crystals. The preparation and characterization of supramolecular liquid crystals, obtained through hydrogen bonding interaction of complementary molecules, has been extensively studied in the last 10 years [7,8].

Recently a wide class of supramolecular liquid crystals were obtained by mixture of dimeric liquid crystals with set of non-mesogenic or mesogenic nanoparticles with different sizes and

CONTACT Minko Petrov mpetrov@issp.bas.bg
This paper was originally submitted to *Molecular Crystals and Liquid Crystals*, Volume 632, Proceedings of the 13th European Conference on Liquid Crystals (ECLC 2015)
Color versions of one or more of the figures in the article can be found online at www.tandfonline.com/gmcl.

shapes [8]. In such produced composite states, the liquid crystal serves as a matrix with ability to impose its inherent high ordering to the bulk ordering of the mixture. The different class of nanoparticles, depending on the character ant the strength of their interactions with the LC matrix, causes a system of mixtures with various optical and electrooptical properties, and aiming to enhance the electrical and optical response of the mixture, including fast relaxations and low-electric field excitation, both necessary for the contemporary photonic devices. Carbon nanotubes are between the most used as doping agent in the liquid crystal matrix, aiming to improve the electrooptical and ordering properties of a set of liquid crystal materials [9–17]. One of the most effective in this direction is the mixture of dimeric LC nOBA, partially the homologue 7OBA, with single walled carbon nanotubes (SWCNTs). 7OBA in the pristine state is achiral LCs displaying the achiral nematic and smectic C states. In the mixture 7OBA/ SWCNTs we indicated [18] that a set of chiral (chiral N^*, ferroelectric smectic C (C^*), reentrant N^*_r and the unique low-temperature ferroelectric smectic C_G (theoretically predicted by de Gennes [19], experimentally confirmed in [20–22] and theoretically described in [23,24] for high-molecular bent-core LCs) appear at cooling of the composite from the isotropic (I) LC state, which is with 4 degrees lower than that of the pristine 7OBA (from 146°C to 142°C). As was indicated in [18], on the base of the pyro-electric method, the ferroelectric polarization value $\boldsymbol{P}$ was estimated to be about 100nC/cm^2. In addition the direction of the polarization vector was indicated (unlike that of the C^* which lays in the smectic layer's plane) which point out of the layer plane ($\mathbf{P}_{out}$). This direction allows the polarization to keep different from zero even in the bulk, similarly to the polarization in the solid state ferroelectric and as a result provokes the lowest possible symmetry-triclinic, as predicted in [19] for smectic C_G. By mirotextural polarization and electrooptical analyses it was indicated that this phase is with two handedness chiral character, fluid in the layer's plane and optically biaxial [18]. So the lowest macroscopic symmetry of the mixture 7OBA/ SWCNTs, gives rise to idea this strong symmetry reduce to be search on a local molecular level. Any more the distruction of the cyclic dimer (breaking of the one or both linear hydrogen bonds) by external action (usually thermal) presume an local molecular symmetry decrease.

A model of the local molecular symmetry decrease and subsequently the macroscopic one will be the goal of the present work. Fundamentally, this model lies at the root of deformation of the dimer ring and as a whole of the dimeric molecule under the action of the SWCNTs field. For the explanation of the dimer ring conformations we can use the investigation of hydrogen bonding state using polarization FT-far infrared spectroscopy (FT far IR spectroscopy −200–30 cm $^{-1}$[25] in combination with micro-Raman polarization one. The microstructure analysis on a molecular level requires the recognition of the hydrogen bonded state, since the linear hydrogen bonds are basic molecular structure elements in dimer LC system.The unusual physical properties of dimer are connected with the both structure characteristics: hydrogen bond dynamics and the closed dimer, open dimer and monomer concentrations at temperature variation [26]. For that purpose, we will use the sensitive to the hydrogen bond state method-the Fourier transformed infrared (FT-IR) spectroscopy in the middle and the far regions-mFT-IR and far FT-IR respectively. In order to analyze the static equilibrium concentrations of different molecular forms of nOBA at temperature cooling of the pristine 7OBA we use the result of mFT-IR spectroscopy, 1700 cm $^{-1}$ in [26], while for the analyze of the hydrogen bonded state we will use far mFT-IR [25]. The microtexture polarization analysis, widely described in [18] also will be used.

2. Experimental results and discussion

For the goal of the present work we used 7OBA supplied by Sigma-Aldirch (Product of Japan). This material is the most chemically stable within the homologues range of the p,n, alkyloxybenzoic acids, since the strength of the linear hydrogen bond of this liquid crystal (20 kJ. mol^{-1}), is two times bigger than those of 8,9OBA ($\approx$10 kJ mol^{-1}). The phase transition temperatures of the pristine 7OBA at cooling are: isotropic I$\rightarrow$nematic N-146°C; N$\rightarrow$smectic C(S_C) −98°C and $S_C\rightarrow$solid state (Cry)-92°C. We realized the mixture 7OBA/SWCNTs using an optimal, for the chiral and ferroelectric states induction, concentration $c = 0.01$ wt%. Purified SWCNT with diameters in the range 1.2–1.4 nm and an aspect ratio of 20–2000, assembled in thin bundles of >2 μm length, produced by arc discharge at Hanwha NanoTech Co., Ltd., were used as purchased. For the microtextural polarization analysis we used the known liquid crystal cell (LCC) preparation, where the substrates are glass plates covered with ITO rubbed layer, in order to reach a LC bulk ordering. The cell thickness of the sample was d=8 μm. As was indicated in [18] the chiral induction was more effective due to both thin cell and good orientation in accordance with an optimal concentration. This effect determines the choice of these experimental parameters. We remind (see [18]) that at these experimental conditions the induced chiral and ferroelectric states at cooling are: I$\rightarrow$N, N$\rightarrow$N*, S_C*$\rightarrow N_r$*, N_r*$\rightarrow C_G$, where N*-chiral nematic, S_C*-ferroelectric smectic C, N_r*-reentrant chiral nematic and C_G-low-temperature smectic C_G state. We concentrate on the low-temperature smectic C_G state, which appears at 86°C at cooling.

By optical microtextural polarization analysis of C_G state at very slow cooling of the sample 7OBA/ SWCNTs (0.1°Cmin^{-1}), starting from the I phase (142 °C), one observes domains, which grow as fractal nuclei and coalesce into large areas with opposite optical rotation (distinct circular dichroism) Fig. 1. At sample rotation in either direction, the red color turns into green and vice versa. Any more at the transition N_r*$\rightarrow C_G$ one also observes a change in fluidity and the texture appears as a colored mosaic texture with equal left-and right-handed helices. Thus one found domains that have opposite director orientations, and hence different handedness, expressing different colors and brightness.These optical characteristics indicate chirality and biaxiality of the LC mixture. Furthermore, such optical behaviour requires a macroscopic symmetry change (symmetry reduction) promoted by the local molecular symmetry decrease. Unlike the conventional S_C phase of pristine 7OBA, where the open dimers

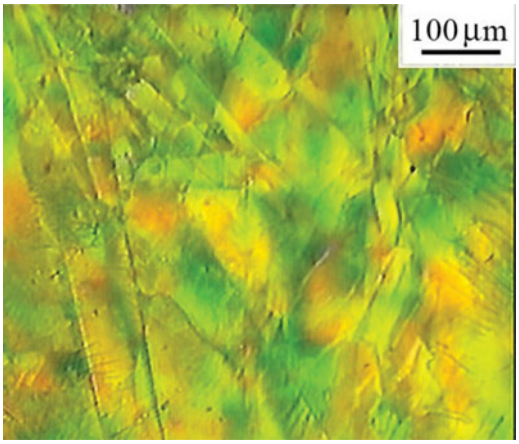

Figure 1. Colored mosaic C_G texture with equal left- and right-handed helices.

can only undergo twisting, the observed combination of chirality and biaxiality implies a loss of the linear shape of the LC molecules.

Summarizing, the dimeric liquid crystal 7OBA/ SWCNTs mixture, at cooling from I phase, exhibits a consecutively a local molecular symmetry reductions, leading to a macroscopical ones as follows: from symmetry $D_{\infty\nu}$ (chiral nematic N*) to symmetry C_2 (S_C*-ferroelectric smectic C with two second order optical axes) to symmetry $D_{\infty\nu)}$ (N_r*) to the lowest triclinic symmetry C_1 (smectic C_G). We remind that the lowest triclinic symmetry, characteristic for the layered smectic states, expresses an optical complex geometry, where none of the principle axes of the second rank tensor, characterizing the orientational order, makes an angle of 0° or $\pi/2$ with the smectic layer's planes. This strong local molecular symmetry decrease, yielding both bi-axiality and chirality, can be realized only, when an induced by dimer conformation local polarization, or polar vector $\boldsymbol{P}$ bound up with the LC director $\boldsymbol{n}$, points out of the smectic layer's planes. The out-of-smectic-layer-plane polarization $\boldsymbol{P}_{\text{out}}$, is the ground characteristic of the smectic C_G phase and depicts the lowest triclinic symmetry, predicted in Ref. [19]. So the smectic C_G type observed here is a chiral phase, formed due to a symmetry reduction in each distinct 7OBA molecule and we assume this to occur by adopting the bent-dimer molecular shape. The necessary energy for this slight deformation can only come from an interaction with the SWCNTs component of the 7OBA/ SWCNTs composite, which represents the only difference between pristine 7OBA and the mixture. Such microtexture and thermal analyses hints for a bending form of the dimer ring of 7OBA in the presence of the SWCNTs.

To understand the mechanism related with the formation of local molecular bent geometry, from initially linear hydrogen bonding dimers, we must to study the competing processes appearing between the intermolecular forces causing both the hydrogen bonding or destruction of the dimer ring, with the forces provoked by the aromatic interactions between the LC benzene rings and the nanotube's aromatic hexagons. For this purpose, we apply both polarization FT far IR spectroscopy (below 100 cm^{-1}) and microRaman spectroscopy. In order to analyze the spectral results, necessary for the smectic C_G model, both intra (concerning the internal degree of the freedom of the molecule, meaning the hydrogen bond states) and intermolecular between dimer ring and nanotube aromatic hexagon interactions follow to be studied.

Let us describe the qualitative model of the low-temperature smectic C_G state appearing in the 7OBA/ SWCNTs mixture. Before that we are going to analyze the structure and the geometrical parameters of the initially non-deformed closed dimer (Fig. 2), expressing the dimer ring of the dimeric LC state.

As is seen from the figure, and on the base of the chemical AB INITIO MO calculation [27], adapted for the large and complex molecules, like that of 7OBA, the structural liquid crystal unit is a combination of dimer ring (two linear hydrogen bonds provoking a cyclic closed dimer) and alkyl chains expressing two flexible parts-centers-the dimer ring and the alkyl chains. The geometrical parameters, including bond angles, as well as bond lengths, magnitudes were presented in [28], using x-ray analysis. In [27] the estimation of energy of bonding, the polarizability and some thermodynamical parameters, important to understand relation between the internal and inter molecular parameters was made for 7OBA.

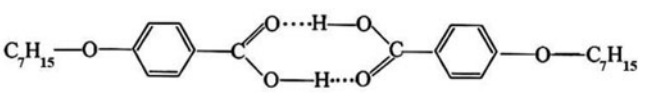

Figure 2. The structure of the constituent molecule of 7OBA.

Some of these structural parameters (dimensions are in good correspondence with X-ray data [28]) are as follows: Monomer: $r_{C=O}$=1.2202 Å, $r_{C\text{-}O}$ = 1.3934 Å, $r_{O\text{-}H}$ = 0.9896 Å, angle $\gamma_{O\text{-}C=O}$ = 121.26° (angle between C = O and C−O groups);Closed Dimer: $r_{O\ldots H}$ = 1.5024 Å, $r_{C=O}$ = 1.2385 Å, r_{C-O} = 1.3521 Å, r_{O-H} = 1.0120 Å, angle $\gamma_{O\text{-}C=O}$ = 123.82°;Open Dimer: $r_{O\ldots H}$ = 1.6761 Å, $r_{C=O}$ = 1.2222 Å, r_{C-O} = 1.3798 Å, r_{O-H} = 0.9942 Å, angle $\gamma_{O\text{-}C=O}$ = 122.71°. These parameters depict the disposition of the bonds participating in the vibrational spectra characteristic for the dimer ring. It is seen that there is a small variation of the geometrical parameters forming the different molecular forms. Significant difference, however, in the energy and the dipole moment values exists when the three fundamental dimer forms appear. Thus, for 7OBA, the dipole moments μ in D (Debye) are 2.2643D for monomers, 0.0418D for the closed dimer and 4.7716D for the open dimers [27]. The dipole moment value of the closed dimer, confirms the logical assumption to be approximately zero. In geometrical presentation, it means two approximately equal parallel dipoles, with opposite directions. In the physical sense $\mu_{dim} \approx 0$ reflects the compensative role on μ of the closed dimer formation, implying that the molecule transforms from dipole (monomer) into quadrupole dielectric state. The calculated energies (ΔE) [27] of transition between monomer, closed dimer and open dimer of 7OBA or specially the the energy of a linear hydrogen bond in the closed dimer is $1/2\Delta E_{mon\rightarrow dim}$ and is−24 kJ.mol^{-1} in good correspondence with that measured in [29].

Consequently, in the frame of one bulk oriented liquid crystal system, in pristine or composite form, there are two factors, which influence local orientation and are decisive for hydrogen bond breaking and formation. The first one is the order parameter $\langle P_2 \rangle$ and the second is the orientation imposed by boundaries or by external e.g electric or magnetic fields. The first factor is pure thermodinamic quantity and exists permanently in the LC state, while the second can be applied or not.

Going to explain the dimer ring conformations, which are in the base of the local molecular symmetry reduction, we use the investigation of hydrogen bonding state in non- exited and exited by the introduce in the system SWCNTs states, using FT-far infrared spectroscopy. The details of the applying and result interpretations related with that spectroscopy see in [25].

Long ago the IR spectroscopic investigations of systems with hydrogen-bonded molecules have been directed mainly towards derivatives of benzol dicarboxylic acid carboxylic acids phenol and benzoic acid [30–36]. The IR spectra of these compounds have been studied in the 4000–700 cm^{-1} region. Late [25] the studies in the range 200–30cm^{-1}, was applied in order to explain the vibrations spectra of the complex dimeric LC molecules like 7OBA.

The dimer structure $(R-CO-OH)_2$ (Fig. 2) has more than 20 internal vibrations. Only six, frequencies, however, can be assigned to hydrogen-bond vibrations or intermolecular vibrations, involving motion of the hydrogen bond. These vibrations, considered as Cartesian displacements, may be described as hydrogen-bond stretching vibrations, in plane or out-of-plane hydrogen-bond bending vibrations or twisting vibrations [25]. For the information about the hydrogen bonding in dimer molecules and hydrogen bonding state, with temperature action variation or SWCNTs action, we used the FT far-IR spectroscopy over the region 100–30 cm^{-1}. FT-IR transmittance spectra we record at both polarizations of the incident light, with the electric vector ***E*** parallel (*p*) and transverse (*s*) to the director ***n*** of the oriented LC system. For investigation of hydrogen bonded OH state, we insert the sample between two quartz plates using FT-Bruker IFS88 spectrometer, with a spectral resolution 0.05 cm^{-1} and assigned different OH bands vibrations frequencies (ν_{OH}). The temperature dependence of the most intense and pronounced spectral bands for *p* and *s* polarization we indicate in Fig. 3.

In the figure we assign the next IR active ν_{OH} vibrations, respectively 64 for *s* polarization, and 40, 60 and 80cm^{-1} for *p* polarization at a temperature 90°C, where the monomers

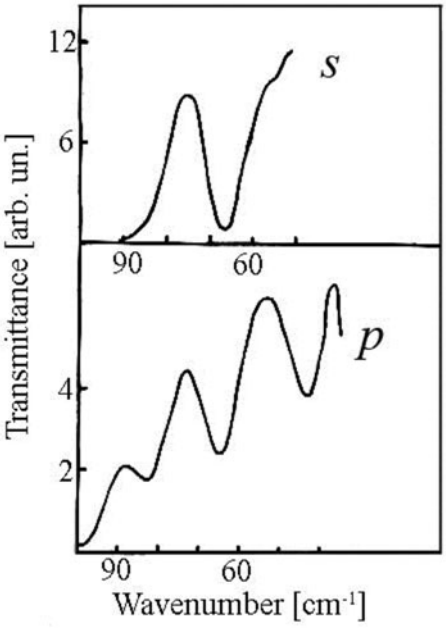

Figure 3. The FT far IR spectra at *s* and *p* polarizations.

disappear and only closed or open dimers retain (see [26]) and is the temperature region where the smectic C_G exists and develops. Consequently, the spectral bands depicted in Fig. 3 are due to the intra-molecular hydrogen-bond deformation vibrations. Such vibrations, because of their low frequencies and large anharmonicity, correspond to a set of absorption bands indicating transitions between fundamental and excited vibrational states of the hydrogen bonds.

As already mentioned, the dimer molecules are molecular quadrupoles due to the two central H-bonds with opposite electric dipoles. One, however, can impose a dipole approximation, assuming the positive and the negative charges of the absorbing dimeric LC to segregate, following their distribution centers. In such way the ensemble of dimer molecules is a supra molecular LC system with an equivalent transition dipole moment $\boldsymbol{P}$, which can rotate around the C-C molecular axis and in vibrational spectroscopy sense is considered as an oscillator accepting the dominating IR active vibrations, stretching, in plane and out of dimer ring plane bending and twist around C-C axis. As indicated above the approximately zero dipole in closed dimer (0.0418D) after the transition to open dimer state obtain a bigger (4.7716 D) transition dipole moment values. Simultaneously, such polar vector $\boldsymbol{P}$ or equivalent transition dipole moment $\boldsymbol{P}$ expressing also the polar director, indicating the intra-molecular degree of freedom or conformational order parameter, deviates by an angle β from the long molecular axis of the non-exited dimer Fig. 4. This figure present the geometry of the polar vector deviation and depicts the dimer ring bending, quantified by the dimer bending kink vector $\boldsymbol{m} \sim \boldsymbol{n_1} \times \boldsymbol{n_2}$ where $\boldsymbol{n_1}$ and $\boldsymbol{n_2}$ are the unit vectors pointing along the two wings of the dimer. As a result, at a realized bending of the dimer ring, $\boldsymbol{n_1}$ and $\boldsymbol{n_2}$ present two local directors both including angle with the director $\boldsymbol{n_0}$ of the initially oriented dimeric LC system. Therefore, this is the geometry depicting the conformational order parameter in the conformed by external actions dimeric system.

Consequently, the dipole moment is a function of the vibration coordinates. The dimer molecular ensemble can be considered also as an oscillator of absorbance. The anisotropy of

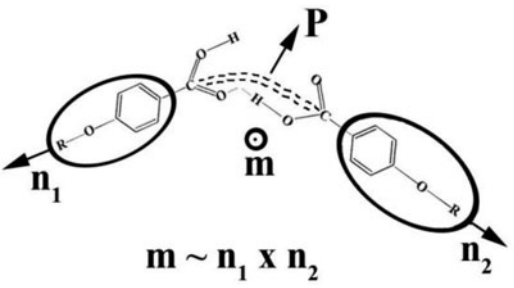

Figure 4. The transiton polar dipole P in bend dimer.

the optical absorption demonstrated by polarization IR analysis is related to the order parameter $\langle P_2 \rangle$ by the equation [37]:$\langle P_2 \rangle = N - 1/N + 2(1 - 3/2 sin^2 \beta)^{-1}$ where $N = D_{||}/D_{\perp}$ is a dichroic ratio and $D_{||}$ and $D_{\perp}$ are optical densities for IR *p* and *s* light propagation parallel and perpendicular to $\boldsymbol{n}$ respectively. The values of $D_{||}$ and $D_{\perp}$ we obtained from the well known formula [37] $D = log(I_o/I_1)$, where I_o and I_1 are the intensities of the incident and the transmitted light, respectively.Thus for the s bands ν_{OH}=82 cm^{-1} of 7OBA for p polarization and $\langle P_2 \rangle$ 0.35 at 100°C [25], β=11°. Thus one accepts that such an oscillation is a hydrogen bond stretching vibration. For the bands $\nu_{OH} = 68$ cm^{-1} at *s* polarization this angle is 60 degrees. It is interesting that the spectral vibration frequencies of the composite 7OBA/SWCNTs keeps the same character stretching, bending in and out of the dimer plane and twist, but due to the dichroic ratio value change the angle β increases from 60 to 74 degrees, thus near to the perpendicular with the respect to the C-C axis vibration. We note that the spectral band of the composite are rather diluted with respect to those of the pristine 7OBA. The new geometry of the vibration direction at the composite, however, hints for a significant enhance of the bend of the dimer and the whole dimeric molecule. So, by FT-far IR analyzes one can detect the hydrogen bond variation, which follows the process of chiralization providing in the 7OBA/SWCNTs composite a domination of the vibration perpendicular to the dimer axis-*s* polarization. Because of the freedom of the oscillator $\boldsymbol{P}$ to rotate around all the axes these bands indicate bending in-and out-of-plane hydrogen bond vibration.The IR active frequency $\nu_{OH} = 42$ cm^{-1}, corresponding to *p* polarization, indicates that at such low frequencies the OH vibration is of a twisting character (rotation around O-H..O axis).

Thus for the temperature range where the smectic C_G state can be induced in the 7OBA/SWCNTs mixture, the dominating OH vibration is $\nu_{OH} = 63$ cm^{-1}, which indicates bending in-and out-of-plane hydrogen bond vibration. One notes, that all the spectral bands are relatively broad and have a complicated structure. Furthermore, there is a phase difference between the oscillations of the dipole moment $\boldsymbol{P}$ and the exciting electric field $\boldsymbol{E}$. Together with the thermal motions of the atoms, these factors give rise to one continuous distribution of the frequencies centered at ν_o corresponding to I_{max}. The extreme broadness of the spectral bands arises from a number of factors: k_BT energy; the large number of molecules in exited vibrational states; and mixtures of different hydrogen-bond configurations and molecular motions. As the temperature decreases more normal band-widths evolve due to the minimization of the above factors.

Let us analyze the Raman active spectral vibrations of the composite 7OBA/SWCNTs presented in Fig. 5

We performed preliminary Raman measurements of the mixture in the low-frequency region at room temperature. Fig. 5 presents such Raman spectra of 7OBA/SWCNTs and 7OBA/PFOA. PFOA is perfluorooctanoic acid. In the 7OBA/SWCNTs spectrum, there are low

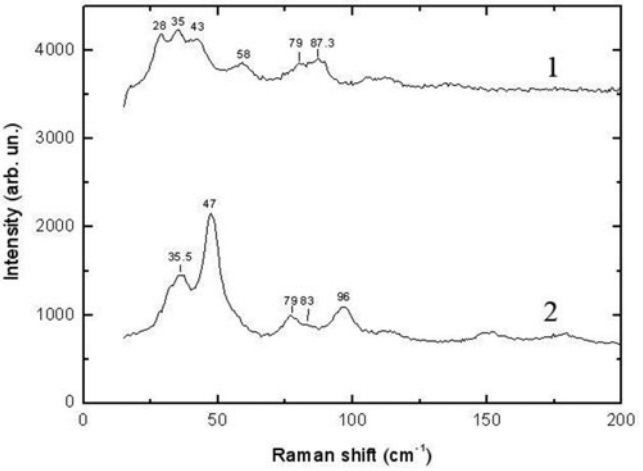

Figure 5. Raman scattering band of the 7OBA/SWCNTs curve1. Curve 2 present the 7OBA/PFOA spectra aiming comparison.

frequency bands (28–43 cm^{-1}, 58 cm^{-1} and 79–88 cm^{-1}), which well correspond to the three principal vibrations detected in the IR spectra (42 cm^{-1}, 63–68 cm^{-1} and 82 cm^{-1}), arising from H-bond twisting, bending and stretching, respectively. On the contrary, the sample containing PFOA, which forms a H-bond with one 7OBA monomer itself, exhibits a completely different low-frequency spectrum. We therefore attribute the three low-frequency bands of 7OBA/SWCNTs to twisting, bending and stretching of either opened or bent dimers aligned by the interaction with the SWCNTs in the C_G phase, and preserving this alignment in the solid (Cry) phase, due to the paramorphic effect. From a comparison with the corresponding IR band a general softening of the bending and twisting vibrations is obvious. We explain this with the argument that these vibrations can be regarded in some general sense as soft modes for dimer bending and opening takes place through displacements along the pertinent vibrational coordinates. On the other hand the development of the single lines in the IR spectra into bands with fine structure is a consequence of the symmetry decrease of the 7OBA molecule and indicates the interaction with the SWCNTs.

Besides this important effect of the vibration softening hinting for dimer bending in the frame of dimer ring structure, the Raman spectra in the range of 100–300cm^{-1} (see [38]) indicates a π - stacking interactions between SWCNTs (carbon aromatic hexagon) and liquid crystal molecules in its benzene core part. As was indicated this stacking up interaction due to the π - π interaction of the molecular electronic orbital of the both aromatic-like interaction of the dimeric LC molecule and the oriented by the liquid crystal matrix carbon nanotubes. In the aspect of the competition between the forces promoted by these intra and intermolecular interaction, and on the ground of the dominating bending (s polarization vibration) one can conclude: that both (in and out of dimer ring plane) perpendicular to the molecular optic axis forces are in coordination with the π - π electronic interaction, thus promoting a local molecular bending (bent dimer) and in consequence causing local and macroscopic symmetry decrease. Besides, the bent dimer, due to the separation of the director $\boldsymbol{n}$ characterizing non-excited one axial LC optical state, into local $\boldsymbol{n_1}$ and $\boldsymbol{n_2}$ optical axes accepts bi-axiality and further due to the IR indicated twist vibration easy obey the typical for the ferroelectrics helix formation.

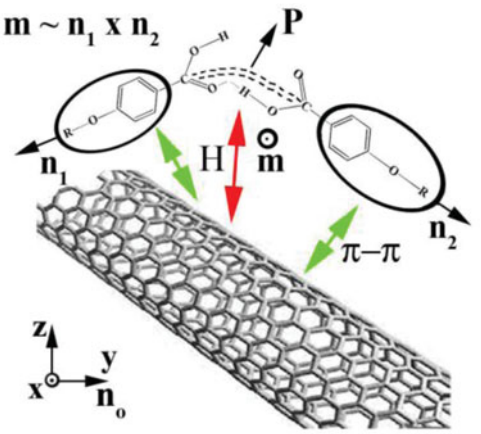

Figure 6. The molecular model of the interaction 7OBA matrix and SWCNT. H indicates the induced by s polarization H-bonding vibration, co-linear with the electronic π-π interaction between 7OBA benzenes and SWCNT carbone hexagones. $\boldsymbol{n_o}$ indicates the imposed by the surfaces planar orientation.

Such local molecular symmetry decreases presume a macroscopic symmetry decrease characteristic for C_G. In the Fig. 6 a possible qualitative molecular model of the bulk interaction of the 7OBA LC matrix and the near-by SWCNT structure unit is depicted. H indicates the induced by the bending H-bonding vibration detected by *s* IR light polarization. The direction of this *s* IR vibration is collinear with the stacking Raman vibration detecting the electronic π-π interaction between the LC benzenes and the carbon hexagons of the SWCNTs causing the LC dimer ring to bend and further to promote a multitude of sterically grazed bent dimers. As a result of this nanoscale process, a macroscopic electrical polarization $\boldsymbol{P}$ arises, which is characteristic for ferroelectric LC states.

Such dimer conformation, due to the minimization of the free energy and the smectic order establishing in the low-temperature region of the dimeric LCs 7OBA where the tilt angle, with respect to the layer's normal arises, initiates an peculiar short and long range smectic ordering and gives a hint for bi-tilted smectic state, which follows to be detected in future very delicate X ray experiments

In Figure 7 we indicate such a possible geometry expressing both chirality and helicity on a molecular level, as well as a bi-axiality, all of them recognized also by the mcrotextural polarization analysis.

Accepting such geometry we can depict the system. The angle ω defines the tilt of the molecular long axis l of the bent (banana shaped) dimer (transferring the two ends of the dimer) with respect to the layer's normal $\mathbf{N}\equiv$Z. This geometry forms the kink (clinic) component of the smectic state. The angle δ (leaning angle) depicts the rotation of the tilt bent dimer plane (boomerang) about l and provokes situation typical for the tilted smectics, where the polarization vector $\boldsymbol{P}$ direction could be perpendicular, parallel or oblique (out of layer's plane polar vector $\boldsymbol{P_{out}}$) with respect to the tilt plane. In this manner a series of ferroelectric states, including C_G, can growth. The values of $0 > \delta < \pi/2$ ensure the leaning component of the bi-tilted system, which in accordance with the kink ones, characterize the low-temperature smectic C_G phase and the lowest triclinic C_1 symmetry. The polarization vector thus has two components: one is in the layer plane and the other one is an out-of-plane component.

As a result of this nanoscale process, a macroscopic electrical polarization arises which is characteristic for ferroelectric LC states. Considering that this interaction significantly lowers the local (nanoscale) and the macroscopical symmetry, we find evidence for the smectic C_G

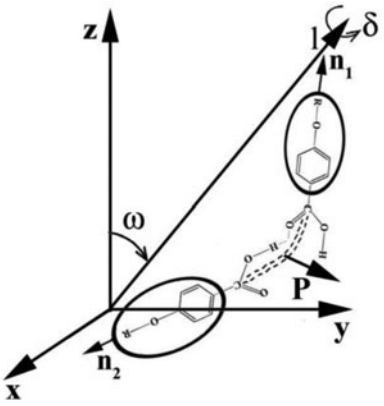

Figure 7. Bi-tilted bent dimer smectic orientation. The layer's normal **N** coincides with z. ω is the smectic tilt angle of the molecular long axis l (clinic) and δ is the leaning angle.

phase with the lowest triclinic symmetry predicted by De Gennes [19].This is also a variant of demonstration of the C_G structure for a material having fluid layers with internally stabilized triclinic symmetry, and substantial coherent molecular tilt in two Euler angles, giving an optical dielectric tensor with none of the principal axes parallel or normal to the layer plane - C_1 symmetry. The result hints at a close similarity between the optical properties and symmetry of high molecular bent-core and low-molecular bent dimers (see [20–24]).

Thus following the succession of the achiral and chiral phase appearance, at temperature decrease, we established general symmetry reduction in the dimeric LC system in pure and nanocomposite states manifested from achiral state, characteristic for the pristine 7OBA substances, in the N and S_C states (with $D_{\infty h}$ and C_{2v} symmetry), to chiral low-symmetric states, including ferroelectric $S_C{}^*$ with C_2 symmetry and ferroelectric smectic C_G with the lowest C_1 triclinic one.

Finally, this qualitative model of the low-molecular dimeric liquid crystals, arises as a necessity to explain the first observed and detailed described in [18] unique C_G in the low-molecular liquid crystals. These phase was already [20–24] detected in the high-molecular bent-core banana shaped LCs and especially in the B7 bis material. The new point is, however, that, while for the high-molecular bent-core LCs, the molecule is previously bended during the synthesis, the bent form in the low-molecular dimeric LCs e.g. in 7OBA, which is needed for C_G phase induction by symmetry reduction is promoted by the external actions. As was indicated in [18] the ferroelectric polarization value in the 7OBA/SWCNT composite is enough large ($\approx$100nC/cm^2) in order the new optical and electrooptical properties of these material to be attractive. The future experimental and theoretical investigations are directed for the improving and supporting of this model.

3. Conclusion

We model the interaction of the dimeric LC matrix of heptyloxybensoic acid (7OBA) and single walled carbon nanotubes (SWCNTs) in a nanocomposite, which causes a local symmetry decrease on the nanoscale. We present evidence for the impact of this local interaction on the macroscopic LC structure, leading to thermally stable low-temperature ferroelectric smectic phase (smectic C_G). By both FT far IR (200–100 cm^{-1}) and Raman spectroscopy, we confirmed the bent dimer formation, which initiates the new low-temperature ferroelectric phase.

Acknowledgements

The work is supported by the grant DFNI-T02/18. The authors thank Boriana Mihailova and Rositsa Titorenkova for help with the Raman measurements.

References

[1] Bennett, J. M., & Jones, B. (1939). *Chem J. Soc.*, *420*.
[2] Gray, G. W., & Jones, B. (1953). *Chem J. Soc.*, *41*, 79.
[3] Treybig, A., Dorscheid, C., Welssflog, W., & Kresse, H. (1969). *Mol Cryst. Liq. Cryst.*, *10*, 219.
[4] Petermann, D., Lemonnier, M., & Meotert, S. CNRS patent No 820334.
[5] Pershin, K., & Konoplev, V. A. (1992). *Liq. Cryst. (UK).*, *12*, 95.
[6] Jahning, F., & Brochard, F. (1974). *J. Phys. (Fr).*, *35*, 301.
[7] Paleos C.M.and Tsiourvas, D. (2001). *Liq.cryst (UK).*, *28*, 1127.
[8] Kato, T., & Frechet Macromol, J. M. J. (1995). *Symp.*, *98*, 311.
[9] Dierking, I., Scalia, G., & Morales, P. (2005). *J. Appl. Phys.*, *97*, 044309.
[10] Podgornov, F., Suvorova, A., Lapanik, A., & Haase, W. (2009). *Chem. Phys. Lett.*, *479*, 206.
[11] Park, K., Mi Lee, S., Lee, S. H., & Lee, Y. H. (2007). *J. Phys. Chem. C.*, *111*, 1620.
[12] Basu, R., Petschek, R. G., & Rosenblatt, C. (2011). *Phys Rev. E.*, *83*, 041707.
[13] Malik, P., Chadhary, A., Mehra, R., & Raina, K. K. (2012). *J. Mol. Liq.*, *165*, 7.
[14] Basu, R., Boccuzzi, K., Ferjani, S., & Rosenblatt, C. (2010). *Appl. Phys. Lett.*, *97*, 121908.
[15] Basu, R., & Iannacchione, G. S. (2010). *Phys Rev. E.*, *81*, 051705.
[16] Basu, R., Chen, C.-L., & Rosenblatt, C. (2011). *J. Appl. Phys.*, *109*, 083518.
[17] Russel, J. M., Oh, S., LaRue, I., Zhou, O., & Samulski, E. T. (2006). *Thin Solid Films*, *509*, 53.
[18] Petrov, M., Katranchev, B., Rafailov, L. P. M., Naradikian, H., Dettlaff-Weglikowska, L. U., Keskinova, E., & Spassov, T. (2013). *Phys. Rew. E.*, *88*, 042503.
[19] De Gennes, P. G., & Prost, J., *The Physics of Liquid Crystals*, 2nd ed. Oxford University Press: New York, 1993.
[20] Jakli, A., Kruerke, D., Sawade, H., & Heppke, G. (2001). *Phys. Rev. Lett.*, *86*, 5715.
[21] Chattham, N., Korblova, E., Shao, R., Walba, D. M., Maclennan, J. E., & Clark, N. A. (2010). *Phys. Rev. Lett.*, *104*, 067801.
[22] Chattham, N., Korblova, E., Shao, R., Walba, D. M., Maclennan, J. E., & Clark, N. A. (2009). *Liq. Cryst.*, *36*, 1309.
[23] Brand, H. R., Cladis, P. E., & Pleiner, H. (1998). *Eur. Phys. J. B.*, *6*, 347.
[24] Cladis, P. E., Brand, H. R., & Pleiner, H. (1999). *Liquid Crystals Today*, *9*, 1.
[25] Petrov, M., *Optical and Electrooptical Properties of Liquid Crystals Nematic and Smectic Phases*, Nova Science Publishers: New York, 2010.
[26] Petrov, M., Anachkova, E., Kirov, N., Ratajczak, H., & Baran, J. (1994). *J. Mokramerl. Liquids*, *61*, 221.
[27] Bobadova, P., Parvanov, V., Petrov, M., & Tsonev, L. (2000). *Cryst. Res. Technol.*, *35*, 1321.
[28] Bryan, R. F., & Hartley, P. (1988). *Mol. Cryst. Liq. Cryst.*, *154*, 77.
[29] Deloche, B., & Cabane, B. (1971). *Mol. Cryst. Liq. Cryst.*, *19*, 25.
[30] Azima, A., Brown, G., & Mitra, S. S. (1975). *Specrichim. Acta.*, *31A*, 1475.
[31] Stanevich, A. E. (1964). *Opt. Spectrosc.*, *16*, 998.
[32] Stanevich, A. E. (1966). *Opt. Spectrosc.*, *21*, 645.
[33] Jacobsen, R. J., & Brasch, J. W. (1969). *Spectrochim. Acta. Part*, *A.25*, 839.
[34] Bentley, F. F., Ryan, M. T., & Katon, J. E. (1964). *Spectrochim Acta.*, *20*, 685.
[35] Allen, G., Watkinson, J. G., & Webb, K. H. (1966). *Spectrochim Acta.*, *22*, 807.
[36] Colombo, L., & Furie, K. (1971). *Spectrochim. Acta. Part*, *A.27*, 1773.
[37] Eliashevitch, M. A. *Atomnaja I Molecularnaja Spectroscopja*, Nauka: Moskow, 1962. (in Russian).
[38] Scalia, G., Lagerwall, J., Haluska, M., Dettlaff-Weglikowska, U., Giesselman, F., & Roth, S. (2006). *Phys. Stat.sol.(b).*, *243*, 3238.